1 **Title:** Carbon cycling in mature and regrowth forests globally: a macroecological synthesis based on the
2 Global Forest Carbon (ForC) database

3 **Authors:**

4 Kristina J. Anderson-Teixeira[1,2]*

5 Valentine Herrmann[1]

6 Becky Banbury Morgan[1,3]

7 Ben Bond-Lamberty[4]

8 Susan C. Cook-Patton[5]

9 Abigail E. Ferson[1,6]

10 Helene C. Muller-Landau[2]

11 Maria M. H. Wang[1,7]

12 **Author Affiliations:**

13   1. Conservation Ecology Center; Smithsonian Conservation Biology Institute; National Zoological Park,
14   Front Royal, VA 22630, USA
15   2. Center for Tropical Forest Science-Forest Global Earth Observatory; Smithsonian Tropical Research
16   Institute; Panama, Republic of Panama
17   3. School of Geography, University of Leeds, Leeds, UK
18   4. Joint Global Change Research Institute, Pacific Northwest National Laboratory, College Park
19   Maryland 20740, USA
20   5. The Nature Conservancy; Arlington VA 22203, USA
21   6. College of Natural Resources, University of Idaho; Moscow, Idaho 83843, USA
22   7. Grantham Centre for Sustainable Futures and Department of Animal and Plant Sciences, University of
23   Sheffield, Western Bank, Sheffield, South Yorkshire S10 2TN, UK

24 *corresponding author: teixeirak@si.edu; +1 540 635 6546

Summary

Background. Earth's climate is closely linked to forests, which strongly influence atmospheric carbon dioxide (CO_2) and climate by their impact on the global carbon (C) cycle. However, efforts to incorporate forests into climate models and CO_2 accounting frameworks have been constrained by a lack of accessible, global-scale data on how C cycling varies across forest types and stand ages.

Methods/Design. Here, we draw from the Global Forest Carbon Database, ForC, to provide a macroscopic overview of C cycling in the world's forests, giving special attention to stand age-related variation. Specifically, we use 11923 *ForC* records from 865 geographic locations representing 34 C cycle variables to characterize ensemble C budgets for four broad forest types (tropical broadleaf evergreen, temperate broadleaf, temperate conifer, and taiga), including estimates for both mature and regrowth (age <100 years) forests. For regrowth forests, we quantify age trends for all variables with sufficient data.

Review Results/ Synthesis. ForC v3.0 yielded a comprehensive picture of C cycling in the world's major forest biomes. The rate of C cycling generally increased from boreal to tropical regions in both mature and regrowth forests, whereas C stocks showed less directional variation. The majority of flux variables, together with most live biomass pools, increased significantly with stand age. Importantly, there was generally good closure of C budgets, *i.e.,* internal consistency in the *ForC* data.

Discussion. As climate change accelerates, understanding and managing the carbon dynamics of forests is critical to forecasting, mitigation, and adaptation. This synthetic and internally consistent global overview of C stocks and fluxes across biomes and stand ages will help to advance these efforts.

Key words: forest ecosystems; carbon cycle; stand age; productivity; respiration; biomass; global

Background

Forest ecosystems are shaping the course of climate change through their influence on atmospheric carbon dioxide (CO_2; Bonan 2008, Friedlingstein *et al* 2019, IPCC 2018). Despite the centrality of forest C cycling in regulating atmospheric CO_2, important uncertainties in climate models (Friedlingstein *et al* 2006, Krause *et al* 2018, Bonan *et al* 2019, Di Vittorio *et al* 2020) and CO_2 accounting frameworks (Pan *et al* 2011) can be traced to lack of accessible, comprehensive data on how C cycling varies across forest types and in relation to stand history. These require large-scale databases with global coverage, which runs contrary to the nature in which forest C stocks and fluxes are measured and published. While remote sensing measurements are increasingly useful for global- or regional-scale estimates of a few critical variables (e.g., aboveground biomass: Hu *et al* 2016, Spawn *et al* 2020, gross primary productivity, *GPP*: Li and Xiao 2019, Saatchi *et al* 2011), measurement and validation of most forest C stocks and fluxes require intensive on-the-ground data collection.

*including those attempting to benchmark model performance with global data (Clark et al 2017, Luo et al 2012), quantify the the role of forests in the global C cycle (*e.g.*, Pan* et al *2011), or use book-keeping methods to quantify actual or scenario-based exchanges of CO_2 between forests and the atmosphere (Griscom* et al *2017, Houghton 2020).*

Forests in the global C cycle: current and future

A robust understanding of forest impacts on global C cycling is essential. Annual gross CO_2 sequestration in forests (gross primary productivity, *GPP*) is estimated at >69 Gt C yr^{-1} (Badgley *et al* 2019), or >7 times average annual fossil fuel emissions from 2009-2018 (9.5 ± 0.5 Gt C yr^{-1}; Friedlingstein *et al* 2019). Most of this enormous C sequestration is counterbalanced by CO_2 releases to the atmosphere through ecosystem respiration (R_{eco}) or fire, with forests globally dominant as sources of both soil respiration (Warner *et al* 2019) and fire emissions (van der Werf *et al* 2017). In recent years, the remaining CO_2 sink averaged 3.2 ± 0.6 GtC yr^{-1} from 2009-2018, offsetting 29% of anthropogenic fossil fuel emissions (Friedlingstein *et al* 2019). Yet, this sink is reduced by deforestation, estimated at ~1 Gt C yr^{-1} in recent decades (Pan *et al* 2011, Tubiello *et al* 2020), reducing the net forest sink to ~1.1-2.2 Gt C yr^{-1} across Earth's forests (Friedlingstein *et al* 2019).

The future of the current forest C sink is dependent both upon forest responses to climate change itself and human land use decisions, which will feedback and strongly influence the course of climate change. Regrowing forests in particular will play an important role (Pugh *et al* 2019), as almost two-thirds of the world's forests were secondary as of 2010 (FAO 2010). As anthropogenic and climate-driven disturbances impact an growing proportion of Earth's forests (**???**, McDowell *et al* 2020), understanding the carbon dynamics of regrowth forests is increasingly important (Anderson-Teixeira *et al* 2013). Although age trends in aboveground biomass have been relatively well-studied and synthesized globally (Cook-Patton *et al* 2020), a relative dearth of data and synthesis on other C stocks and fluxes in secondary forests points to an under-filled need to characterize age-related trends in forest C cycling. Such understanding is particularly critical for reducing uncertainty regarding the potential for carbon uptake and climate change mitigation by regrowth forests (Krause *et al* 2018, Cook-Patton *et al* 2020). Understanding, modeling, and managing forest-atmosphere CO_2 exchange is thus central to efforts to mitigate climate change (Grassi *et al* 2017, Griscom *et al* 2017, Cavaleri *et al* 2015).

Evolution of forest C cycle research

For more than half a century, researchers have sought to understand how forest carbon cycling varies across stands, including those of different biomes (e.g., Leith, Luyssaert *et al* 2007) and stand ages (e.g., Odum 1969 Odum, Luyssaert 2008). - increasingly refined understanding of the elements of ecosystem C cycles, - standardization of definitions, (which were vague at the time of Odum) - Expanding set of variables, notably including the development of the eddy-covariance technique to measure ecosystem-atmosphere CO_2 exchange (REFS), NEP, soil respiration, Also various techniques for measuring belowground C cycling. - critical review of methods and their sources of errors - Increasing standardization of methods: allometries, which are highly influential to any measurement including woody biomass or changes therein, but until recently have not been standardized - Further standardization made possible through research networks such as ForestGEO (Anderson-Teixeira *et al* 2015, e.g., Lutz *et al* 2018), GEM (Malhi), NEON (Schimel *et al* 2007), or FLUXNET (Baldocchi *et al* 2001, e.g., Novick *et al* 2018).

Alongside these conceptual and methodological developments, there has been a proliferation of measurements across the world's forests. The result of decades of research on forest C cycling is that tens of thousands of records have been distributed across literally thousands of scientific articles –often behind paywalls– along with variation in data formats, units, measurement methods, *etc.* In this format, the data are effectively inaccessible for many global-scale analyses, Data synthesis began,...

To address the need for global-scale analyses of forest C cycling, we recently developed *ForC* (Anderson-Teixeira *et al* 2016, 2018). *ForC* contains published estimates of forest ecosystem C stocks and annual fluxes (>50 variables), with the different variables capturing the unique ecosystem pools (e.g., woody, foliage, and root biomass; dead wood) and flux types (e.g, gross and net primary productivity; soil, root, and ecosystem respiration). These data are ground-based measurements, and *ForC* contains associated data required for interpretation (*e.g.*, stand history, measurement methods). Data have been amalgamated from original peer-reviewed publications, either directly or via intermediary data compilations. Since its most recent publication (Anderson-Teixeira *et al* 2018), *ForC* has grown to include two additional large databases: the Global Soil Respiration Database (SRDB; Bond-Lamberty and Thomson 2010) and the Global Reforestation Opportunity Assessment database (GROA; Cook-Patton *et al* 2020) that also synthesized published forest C data. Following these additions, *ForC* currently contains 39762 records from 10608 plots and 1532 distinct geographic areas representing all forested biogeographic and climate zones. This represents an 129% increase in records from the prior publication (Anderson-Teixeira *et al* 2018).

Biome differences

Forest C cycling varies enormously across biomes... Biome is an artificial categorical distinction convenient for categorizing the world's forests according to major differences in climate and vegetation.

The most important gradient for defining biomes is climate. Since (Humboldt?), it has been recognized that climate plays a dominant role in shaping differences among forests.

Lieth (1973) synthesized differences in NPP across gradients of mean annual temperture and precipitation.

Banbury Morgan *et al* (n.d.)

Recently, machine learning draws on global maps in combination with ground-based data to create global maps of C cycling (e.g., REFS; Cook-Patton *et al* 2020).

4

¹²⁴ While current data and technology allow increasingly fine-scale resolution for understanding differences
¹²⁵ across forests, cateogorization into biomes remains useful for applications where data do not yet support
¹²⁶ robust analysis across finer-scale axes of variation.

Age trends and their variation across biomes

¹²⁸ In 1969, Eugene Odum published ... (Odum 1969). Although the conceptualization of the C cycle in this
¹²⁹ paper is simplistic by current standards, the paper was foundational... (Corman *et al* 2019). ... *(Need for*
¹³⁰ *a synthetic update.)*

¹³¹ In the past *couple of/several* decades, researchers have started asking how age trends–mostly in biomass
¹³² accumulation– vary across biomes. *(look up early work on this–citations in Anderson* et al *(2006))* Anderson
¹³³ *et al* (2006) (**???**) Cook-Patton *et al* (2020) There has been little synthesis of differences in variables other
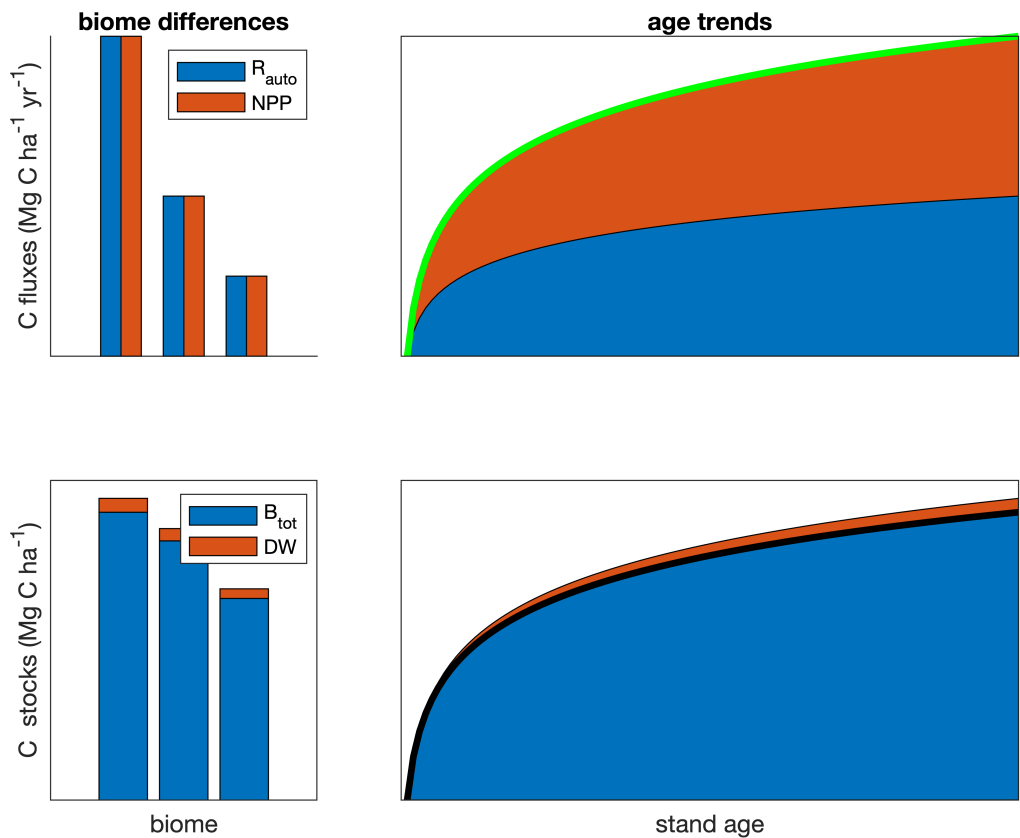¹³⁴ than C stocks or their accumulation rates.

Figure 1 | DRAFT SCHEMATIC.

¹³⁵ Here, conduct a data-based review of carbon cycling from a stand to global level, and by biome and stand
¹³⁶ age, using the largest global compilation of forest carbon data, which is available in our open source Global
¹³⁷ Carbon Forest database (*ForC*; Fig. 2). Our primary goal is to provide a comprehensive synthesis on broad
¹³⁸ trends in forest C cycling that can serve as a foundation for improved understanding of global forest C

¹³⁹ cycling and highlight where key sources of uncertainty still reside.
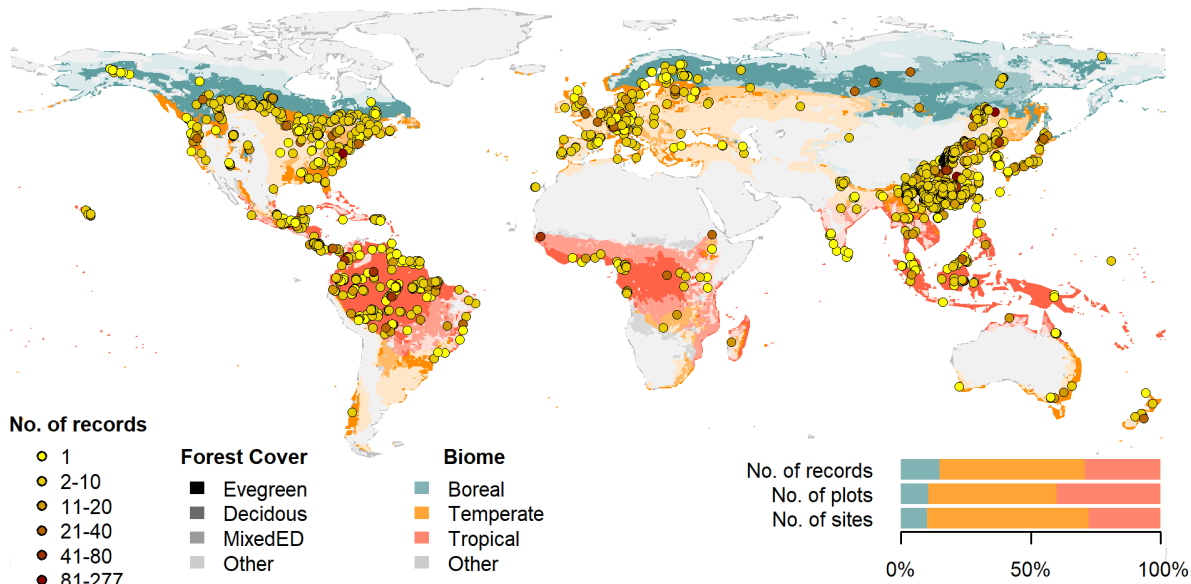

Figure 2 | Map of sites included in this analysis. Symbols are colored according to the number of records at each site. Underlying map shows coverage of evergreen, deciduous, and mixed forests (from SYNMAP; Jung et al. 2006) and biomes. Distribution of sites, plots, and records among biomes is shown in the inset.

Methods/ Design

¹⁴¹ This review synthesizes data from the *ForC* database (Fig. 2; https://github.com/forc-db/ForC;

¹⁴² Anderson-Teixeira *et al* 2016, 2018). *ForC* amalgamates numerous intermediary data sets (*e.g.*, Luyssaert *et*

¹⁴³ *al* 2007, Bond-Lamberty and Thomson 2010, Cook-Patton *et al* 2020) and original studies. Original

¹⁴⁴ publications were referenced to check values and obtain information not contained in intermediary data sets,

¹⁴⁵ although this process has not been completed for all records. The database was developed with goals of

¹⁴⁶ understanding how C cycling in forests varies across broad geographic scales and as a function of stand age.

¹⁴⁷ As such, there has been a focus on incorporating data from regrowth forests (*e.g.*, Anderson et al 2006,

¹⁴⁸ Martin et al 2013, Bonner et al 2013) and obtaining stand age data when possible (83% of records in v.2.0;

¹⁴⁹ Anderson-Teixeira *et al* 2018). Particular attention was given to developing the database for tropical forests

¹⁵⁰ (Anderson-Teixeira *et al* 2016), which represented roughly one-third of records in *ForC* v2.0

¹⁵¹ (Anderson-Teixeira *et al* 2018). Since publication of ForC v2.0, we added the following data to ForC: the

¹⁵² Global Database of Soil Respiration Database (*SRDB* v4, 9488 records; Bond-Lamberty and Thomson 2010),

¹⁵³ the Global Reforestation Opportunity Assessment database (*GROA* v1.0, 10116 records; Cook-Patton *et al*

¹⁵⁴ 2020, Anderson-Teixeira *et al* 2020). We have also added data from individual publications, with a particular

¹⁵⁵ focus on productivity (e.g., **???**), dead wood, and ForestGEO sites (e.g., Lutz *et al* 2018, p

¹⁵⁶ @johnson_climate_2018). The database version used for this analysis has been tagged as a new release on

¹⁵⁷ Github (v3.0) and assigned a DOI through Zenodo (DOI: TBD).

To facilitate analyses, we created a simplified version of ForC, *ForC-simplified*

(https://github.com/forc-db/ForC/blob/master/ForC_simplified), which we analyzed here. In generating

ForC-simplified, all measurements originally expressed in units of dry organic matter (OM) were converted

to units of C using the IPCC default of $C = 0.47 * OM$ (IPCC 2018). Duplicate or otherwise conflicting

records were reconciled as described in Appendix S1, resulting in a total of 22265 records (56% size of total

database). Records were filtered to remove plots that had undergone significant anthropogenic management

or major disturbance since the most recent stand initiation event. Specifically, we removed all plots flagged

as managed in ForC-simplified (13.9%). This included plots with any record of managements manipulating

CO_2, temperature, hydrology, nutrients, or biota, as well as any plots whose site or plot name contained the

terms "plantation", "planted", "managed", "irrigated", or "fertilized". Plots flagged as disturbed in

ForC-simplified (5.6%) included stands that had undergone any notable anthropogenic thinning or partial

harvest. We retained sites that were grazed or had undergone low severity natural disturbances (<10%

mortality) including droughts, major storms, fires, and floods. We removed all plots for which no stand

history information had been retrieved (5.7%). In total, this resulted in 17349 records (43.6% of the records

in the database) being eligible for inclusion in the analysis.

We selected 23 annual flux and 11 C stock variables for inclusion in the analysis (Table 1). These different

flux and stock variables represent different pools (e.g., aboveground biomass, root biomass, dead wood) and

levels of combination (e.g., total net primary productivity, NPP, versus the individual elements of NPP

such as foliage, roots, and branches). Note that two flux variables, aboveground heterotropic (R_{het-ag}) and

total (R_{het}) respiration, were included for conceptual completeness but had no records in *ForC* (Table 1).

Records for our focal variables represented 90.3% of the total records eligible for inclusion. For this analysis,

we combined some of ForC's specific variables into more broadly defined variables. Specifically, net ecosystem

exchange (measured by eddy-covariance; Baldocchi *et al* 2001) and biometric estimates of NEP were

combined into the single variable NEP (Table 1). Furthermore, for NPP, aboveground NPP ($ANPP$),

and the litterfall component of $ANPP$ ($ANPP_{litterfall}$), *ForC* variables specifying inclusion of different

components were combined (*e.g.*, measurements including or excluding fruit and flower production and

herbivory). Throughout ForC, for all measurements drawing from tree census data (*e.g.*, biomass,

productivity), the minimum diameter breast height (DBH) threshold for tree census was $\leq 10cm$. All records

were measured directly or derived from field measurements (as opposed to modeled).

We grouped forests into four broad biome types based on climate zones and dominant vegetation type

(tropical broadleaf, temperate broadleaf, temperate needleleaf, and boreal needleleaf) and two age

classifications (young and mature). Climate zones (Fig. 2) were defined based on site geographic coordinates

according to Köppen-Geiger zones (Rubel and Kottek 2010). We defined the tropical biome as including all

equatorial (A) zones, temperate biomes as including all warm temperate (C) zones and warmer snow

climates (Dsa, Dsb, Dwa, Dwb, Dfa, and Dfb), and the boreal biome as including the colder snow climates

(Dsc, Dsd, Dwc, Dwd, Dfc, and Dfd). Any forests in dry (B) and polar (E) Köppen-Geiger zones were

excluded from the analysis. We defined leaf type (broadleaf / needleleaf) was based on descriptions in

original publications (prioritized) or values extracted from a global map based on satellite observations

(SYNMAP; Jung *et al* 2006). For young tropical forests imported from *GROA* but not yet classified by leaf

type, we assumed that all were broadleaf, consistent with the rarity of naturally regenerating needleleaf

forests in the tropics. We also classified forests as "young" (< 100 years) or "mature" (≥ 100 years or

classified as "mature", "old growth", "intact", or "undisturbed" in original publication). Assigning stands to

Table 1. Carbon cycle variables included in this analysis, their sample sizes, and summary of biome differences and age trends.

Variable	Description	N records records	N records plots	N records geographic areas	biome differences[*]	age trend[†]
Annual fluxes						
NEP	net ecosystem production or net ecosystem exchange (+ indicates C sink)	329	146	88	n.s.	+; xB
GPP	gross primary production ($NPP + R_{auto}$ or $R_{eco} - NEE$)	303	115	84	TrB > TeB $\geq$ TeN $\geq$ BoN	+; xB
NPP	net primary production ($ANPP + BNPP$)	214	112	74	TrB > TeB $\geq$ TeN > BoN	n.s.
$ANPP$	aboveground NPP	343	236	131	TrB > TeB $\geq$ TeN > BoN	+; xB
$ANPP_{woody}$	woody production ($ANPP_{stem} + ANPP_{branch}$)	64	53	37	n.s.	+
$ANPP_{stem}$	woody stem production	217	190	117	TrB > TeN $\geq$ TeB $\geq$ BoN	n.s.
$ANPP_{branch}$	branch turnover	69	59	42	TrB > TeB $\geq$ TeN	n.s.
$ANPP_{foliage}$	foliage production, typically estimated as annual leaf litterfall	162	132	88	TrB > TeB $\geq$ TeN > BoN	+
$ANPP_{litterfall}$	litterfall, including leaves, reproductive structures, twigs, and sometimes branches	82	70	55	n.s.	+
$ANPP_{repro}$	production of reproductive structures (flowers, fruits, seeds)	51	44	34	n.t.	n.t.
$ANPP_{folivory}$	foliar biomass consumed by folivores	20	12	11	n.t.	n.t.
M_{woody}	woody mortality–i.e., B_{ag} of trees that die	18	18	18	n.t.	n.t.
$BNPP$	belowground NPP ($BNPP_{coarse} + BNPP_{fine}$)	148	116	79	TrB > TeN $\geq$ TeB $\geq$ BoN	+
$BNPP_{coarse}$	coarse root production	77	56	36	TeN $\geq$ TrB	n.s.
$BNPP_{fine}$	fine root production	123	99	66	n.s.	+
R_{eco}	ecosystem respiration ($R_{auto} + R_{het}$)	213	98	70	TrB > TeB $\geq$ TeN	+
R_{auto}	autotrophic respiration ($R_{auto-ag} + R_{root}$)	24	23	15	n.t.	n.t.
$R_{auto-ag}$	aboveground autotrophic respiration (i.e., leaves and stems)	2	2	1	n.t.	n.t.
R_{root}	root respiration	181	139	95	TrB $\geq$ TeB	+
R_{soil}	soil respiration ($R_{het-soil} + R_{root}$)	627	411	229	TrB > TeB > TeN $\geq$ BoN	n.s.
$R_{het-soil}$	soil heterotrophic respiration	197	156	100	TrB > TeB $\geq$ TeN	n.s.
R_{het-ag}	aboveground heterotrophic respiration	0	0	0	-	-
R_{het}	heterotrophic respiration ($R_{het-ag} + R_{het-soil}$)	0	0	0	-	-
Stocks						
B_{tot}	total live biomass ($B_{ag} + B_{root}$)	188	157	87	TrB $\geq$ TeB > BoN	+; xB
B_{ag}	aboveground live biomass ($B_{ag-wood} + B_{foliage}$)	4466	4072	621	TrB $\geq$ TeN $\geq$ TeB > BoN	+; xB
$B_{ag-wood}$	woody component of aboveground biomass	115	102	64	TeN > TrB $\geq$ BoN	+; xB
$B_{foliage}$	foliage biomass	134	115	72	TeN > TrB $\geq$ BoN $\geq$ TeB	+; xB
B_{root}	total root biomass ($B_{root-coarse} + B_{root-fine}$)	2329	2298	360	n.s.	+; xB
$B_{root-coarse}$	coarse root biomass	134	120	73	TeN > TeB $\geq$ BoN	+; xB
$B_{root-fine}$	fine root biomass	226	180	109	n.s.	+; xB
DW_{tot}	deadwood ($DW_{standing} + DW_{down}$)	79	73	42	n.t.	+; xB
$DW_{standing}$	standing dead wood	36	35	22	n.t.	n.t.
DW_{down}	fallen dead wood, including coarse and sometimes fine woody debris	278	265	37	n.t.	+; xB
OL	organic layer / litter/ forest floor	474	413	115	n.s.	+; xB

[*] Tr: Tropical, TeB: Temperate Broadleaf, TeN: Temperate Needleleaf, B: Boreal, n.s.: no significant differences, n.t.: not tested

[†] + or -: significant positive or negative trend, xB: significant age x biome interaction, n.s.: no significant age trend, n.t.: not tested

these groupings required the exclusion of records for which *ForC* lacked geographic coordinates (0.4% of sites in full database) or records of stand age (5.7% of records in full database). We also excluded records of stand

age = 0 year (0.8% of records in full database). In total, our analysis retained 76.1 of the focal variable records for forests of known age. Numbers of records by biome and age class are given in Table S1.

Data were summarized to produce schematics of C cycling across the eight biome by age group combinations identified above. To obtain the values reported in the C cycle schematics, we first averaged any repeated measurements within a plot. Values were then averaged across geographically distinct areas, defined as plots clustered within 25 km of one another (*sensu* Anderson-Teixeira *et al* 2018), weighting by area sampled if available for all records. This step was taken to avoid pseudo-replication.

We tested whether the C budgets described above "closed"–*i.e.*, whether they were internally consistent. Specifically, we first defined relationships among variables: for example, $NEP = GPP - R_{eco}$, $BNPP = BNPP_{coarse} + BNPP_{fine}$, $DW_{tot} = DW_{standing} + DW_{down}$). Henceforth, we refer to the variables on the left side of the equation as "aggregate" fluxes or stocks, and those that are summed as "component" fluxes or stocks, noting that the same variable can take both aggregate and component positions in different relationships. We considered the C budget for a given relationship "closed" when component variables summed to within one standard deviation of the aggregate variable.

To test for differences across mature forest biomes, we also examined how stand age impacted fluxes and stocks, employing a mixed effects model ("lmer" function in "lme4" R package; Bates *et al* 2015) with biome as fixed effect and plot nested within geographic.area as random effects on the intercept. When Biome had a significant effect, we looked at a Tukey's pairwise comparison to see which biomes were significantly different from one another. This analysis was run for variables with records for at least seven distinct geographic areas in more than one biome, excluding any biomes that failed this criteria (Table 1).

To test for age trends in young (<100yrs) forests, we employed a mixed effects model with biome and log10[stand.age] as fixed effects and plot nested within geographic.area as a random effect on the intercept. This analysis was run for variables with records for at least three distinct geographic areas in more than one biome, excluding any biomes that failed this criteria (Table 1). When the effect of stand age was significant at p ≤ 0.05 and when each biome had records for stands of at least 10 different ages, a biome × stand.age interaction was included in the model.

To facilitate the accessibility of our results and data, and to allow for rapid updates as additional data become available, we have automated all database manipulation, analyses, and figure production in R (**???**).

Review Results/ Synthesis

Data Coverage

Of the 39762 records in *ForC* v3.0, 11923 met our strict criteria for inclusion in this study (Fig. 2). These records were distributed across 5062 plots in 865 distinct geographic areas. Of the 23 flux and 11 stock variables mapped in these diagrams, *ForC* contained sufficient mature forest data for inclusion in our statistical analyses (*i.e.*, records from ≥ 7 distinct geographic areas) for 20 fluxes and 9 stocks in tropical broadleaf forests, 15 fluxes and 8 stocks in temperate broadleaf forests, 14 fluxes and 7 stocks in temperate conifer forests, and 8 fluxes and 7 stocks in boreal forests. For regrowth forests (<100 yrs), *ForC* contained sufficient data for inclusion in our statistical analyses (*i.e.*, records from ≥ 3 distinct geographic areas) for 11 fluxes and 10 stocks in tropical broadleaf forests, 16 fluxes and 10 stocks in temperate broadleaf forests, 16 fluxes and 10 stocks in temperate conifer forests, and 14 fluxes and 9 stocks in boreal forests.

9

C cycling in mature forests

Average C cycles for mature tropical broadleaf, temperate broadleaf, temperate conifer, and boreal forests $\geq$ 100 years old and with no known major natural or anthropogenic disturbance are presented in Figures 2-5 (and available in tabular format in the *ForC* release accompanying this publication: `ForC/numbers_and_facts/ForC_variable_averages_per_Biome.csv`).

For variables with records from ≥ 7 distinct geographic areas, these ensemble C budgets were generally consistent. That is, component variables summed to within one standard deviation of their respective aggregate variables in all but one instance. In the temperate conifer biome, the average composite measure of root biomass (B_{root}) was less than the combined average value of coarse and fine root biomass ($B_{root-coarse}$ and $B_{root-fine}$, respectively). This lack of closure was driven by very high estimates of $B_{root-coarse}$ from high-biomass forests of the US Pacific Northwest.

10

Figure 3 | C cycle diagram for mature tropical broadleaf forests. Arrows indicate fluxes (Mg C ha^{-1} yr^{-1}); boxes indicate stocks (Mg C ha^{-1}), with variables as defined in Table 1. Presented are mean $\pm$ std, where geographically distinct areas are treated as the unit of replication. Dashed shape outlines indicate variables with records from <7 distinct geographic areas, and dashed arrows indicate fluxes with no data. To illustrate the magnitude of different fluxes, arrow size is proportional to the square root of corresponding flux. Asterisk after variable name indicates lack of C cycle closure.
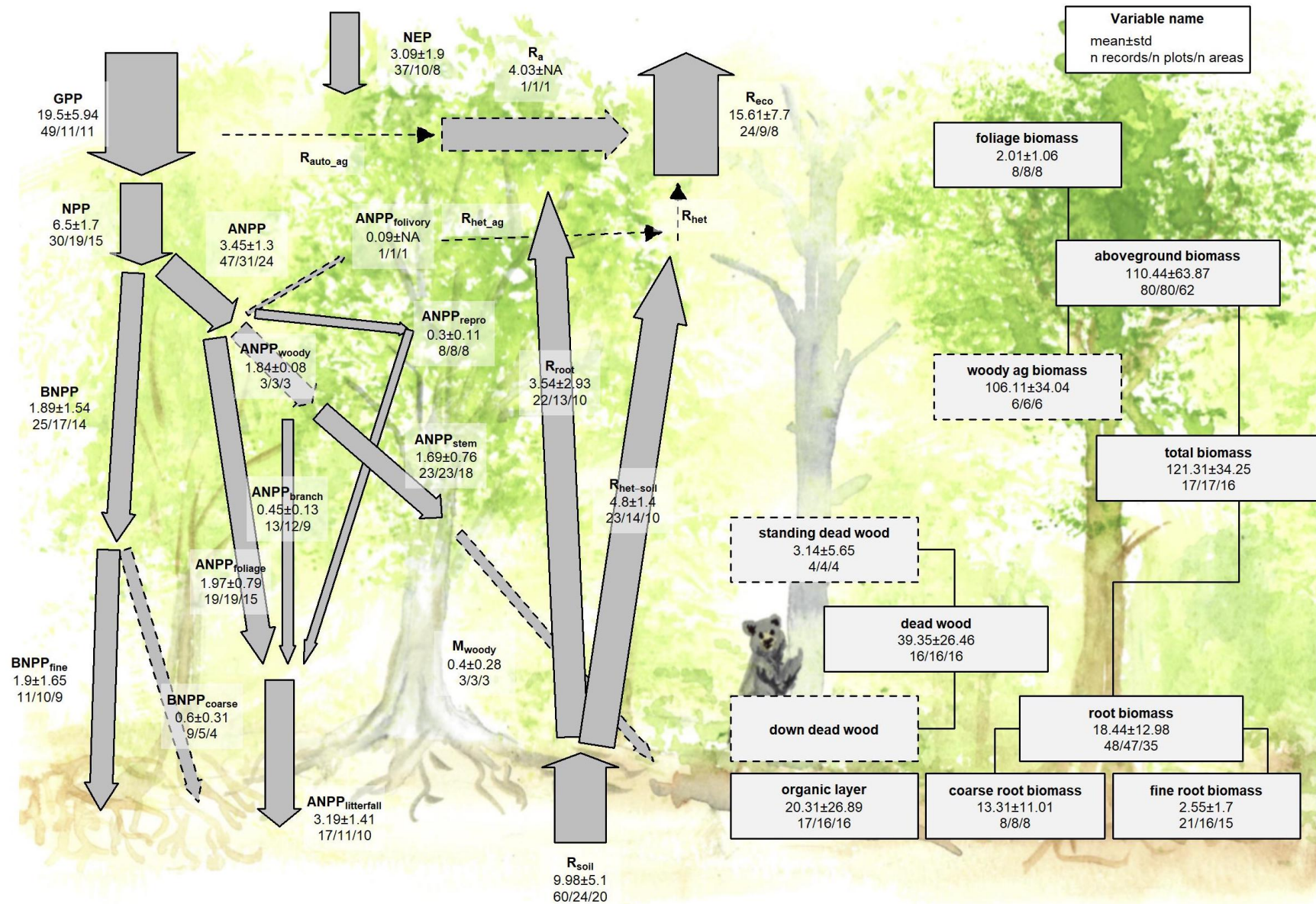
Variable name

mean±std

n records/n plots/n areas

NEP
3.09±1.9
37/10/8

R_a
4.03±NA
1/1/1

R_{eco}
15.61±7.7
24/9/8

GPP
19.5±5.94
49/11/11

R_{auto_ag}

foliage biomass
2.01±1.06
8/8/8

NPP
6.5±1.7
30/19/15

ANPP
3.45±1.3
47/31/24

$ANPP_{folivory}$
0.09±NA
1/1/1

R_{het_ag}

R_{het}

aboveground biomass
110.44±63.87
80/80/62

$ANPP_{repro}$
0.3±0.11
8/8/8

$ANPP_{woody}$
1.84±0.08
3/3/3

R_{root}
3.54±2.93
22/13/10

woody ag biomass
106.11±34.04
6/6/6

BNPP
1.89±1.54
25/17/14

$ANPP_{stem}$
1.69±0.76
23/23/18

total biomass
121.31±34.25
17/17/16

$ANPP_{branch}$
0.45±0.13
13/12/9

$R_{het-soil}$
4.8±1.4
23/14/10

$ANPP_{foliage}$
1.97±0.79
19/19/15

standing dead wood
3.14±5.65
4/4/4

$BNPP_{fine}$
1.9±1.65
11/10/9

$BNPP_{coarse}$
0.6±0.31
9/5/4

M_{woody}
0.4±0.28
3/3/3

dead wood
39.35±26.46
16/16/16

root biomass
18.44±12.98
48/47/35

down dead wood

$ANPP_{litterfall}$
3.19±1.41
17/11/10

organic layer
20.31±26.89
17/16/16

coarse root biomass
13.31±11.01
8/8/8

fine root biomass
2.55±1.7
21/16/15

R_{soil}
9.98±5.1
60/24/20

Figure 4 | C cycle diagram for mature temperate broadleaf forests. Arrows indicate fluxes (Mg C ha^{-1} yr^{-1}); boxes indicate stocks (Mg C ha^{-1}), with variables as defined in Table 1. Presented are mean ± std, where geographically distinct areas are treated as the unit of replication. Dashed shape outlines indicate variables with records from <7 distinct geographic areas, and dashed arrows indicate fluxes with no data. To illustrate the magnitude of different fluxes, arrow size is proportional to the square root of corresponding flux. Asterisk after variable name indicates lack of C cycle closure.

Variable name
mean±std
n records/n plots/n areas

NEP
0.69±1.99
35/12/11

R_a
11.66±3.93
5/5/4

R_{eco}
11.57±3.31
19/10/8

GPP
13.97±4.7
44/13/10

foliage biomass
9.04±3.06
12/12/11

R_{auto_ag}
1.99±NA
1/1/1

NPP
5.2±2.11
22/13/10

ANPP
3.14±1.46
45/24/17

$ANPP_{folivory}$
0.15±NA
1/1/1

R_{het_ag}

R_{het}

aboveground biomass
167.46±177.12
83/71/35

$ANPP_{repro}$
0.14±0.08
3/3/3

$ANPP_{woody}$
2.54±1.39
9/9/8

R_{root}
2.61±1.01
17/6/6

woody ag biomass
315.61±156.4
12/12/10

BNPP
2.03±1.37
17/10/8

$ANPP_{stem}$
1.92±1.01
16/16/12

total biomass
226.58±123.54
8/7/5

$ANPP_{branch}$
0.28±0.18
12/12/10

$R_{het-soil}$
4.36±1.23
14/8/8

$ANPP_{foliage}$
1.7±0.72
13/13/10

standing dead wood
12.83±11.58
3/3/3

dead wood
94.93±28.99
3/3/3

BNPP_{fine}
1.5±0.64
9/8/7

$BNPP_{coarse}$
0.89±0.57
10/10/8

M_{woody}

root biomass*
33.38±38.32
51/51/14

down dead wood

organic layer
18.97±17.85
13/9/7

coarse root biomass
77.56±58.1
16/15/12

fine root biomass
2.23±1.14
10/10/8

$ANPP_{litterfall}$
2.38±0.93
4/4/3

R_{soil}
7.11±2.51
56/26/21

Figure 5 | C cycle diagram for mature temperate conifer forests. Arrows indicate fluxes (Mg C ha^{-1} yr^{-1}); boxes indicate stocks (Mg C ha^{-1}), with variables as defined in Table 1. Presented are mean ± std, where geographically distinct areas are treated as the unit of replication. Dashed shape outlines indicate variables with records from <7 distinct geographic areas, and dashed arrows indicate fluxes with no data. To illustrate the magnitude of different fluxes, arrow size is proportional to the square root of corresponding flux. Asterisk after variable name indicates lack of C cycle closure.
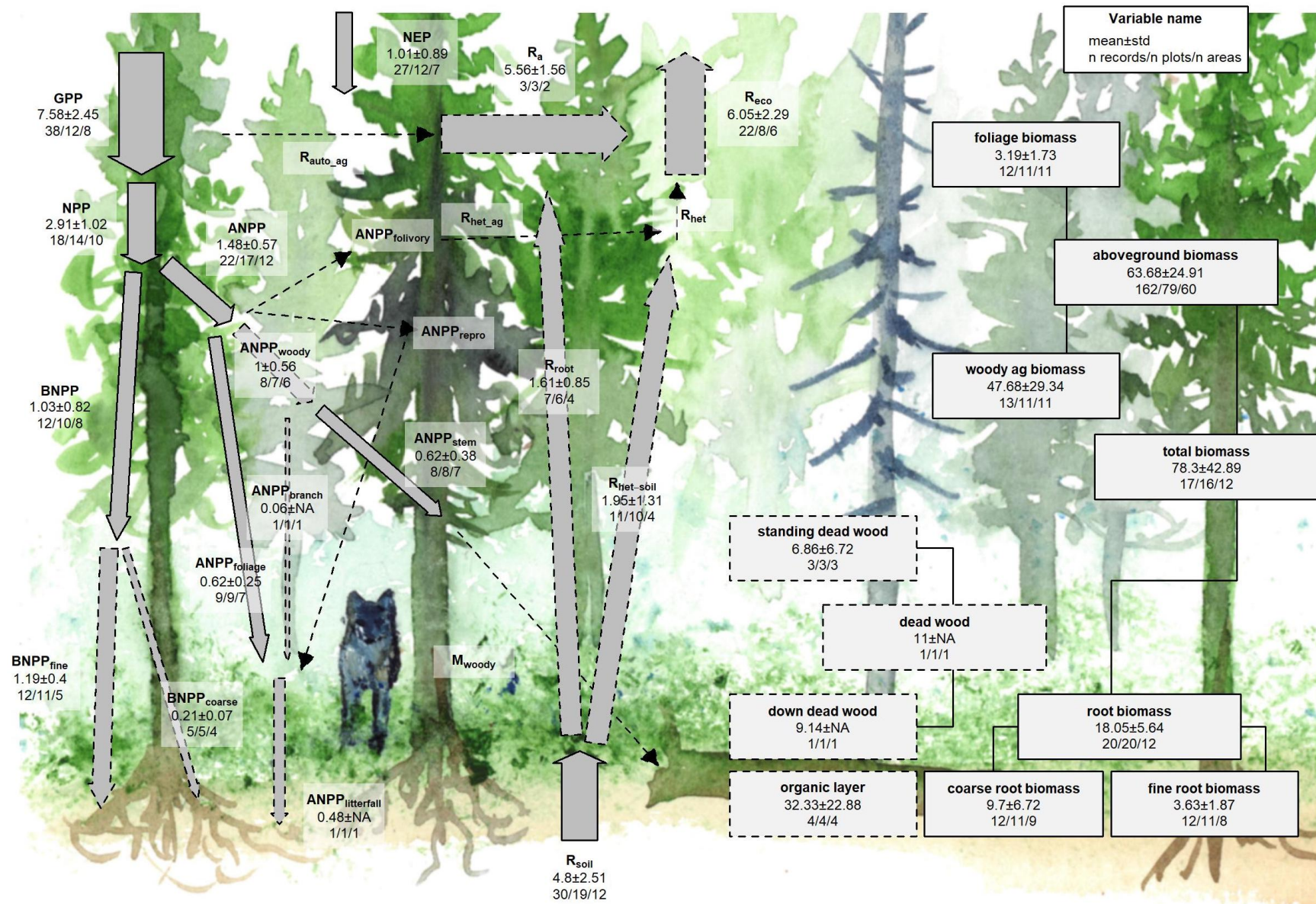
Figure 6 | C cycle diagram for mature boreal conifer forests. Arrows indicate fluxes (Mg C ha^{-1} yr^{-1}); boxes indicate stocks (Mg C ha^{-1}), with variables as defined in Table 1. Presented are mean $\pm$ std, where geographically distinct areas are treated as the unit of replication. Dashed shape outlines indicate variables with records from <7 distinct geographic areas, and dashed arrows indicate fluxes with no data. To illustrate the magnitude of different fluxes, arrow size is proportional to the square root of corresponding flux. Asterisk after variable name indicates lack of C cycle closure.

There were sufficient data to assess mature forest biome differences for 15 flux variables, and significant differences among biomes were detected for 12 variables (Table 1). In all of these cases–including C fluxes into, within, and out of the ecosystem–C fluxes were highest in tropical forests, intermediate in temperate (broadleaf or conifer) forests, and lowest in boreal forests (Table 1, Figs. 7, S5-S19). Differences between tropical and boreal forests were always significant, with temperate forests intermediate and significantly different from one or both. Fluxes tended to be numerically greater in temperate broadleaf than conifer forests, but the difference was never statistically significant. This pattern held for the following variables: GPP, NPP, $ANPP$, $ANPP_{stem}$, $ANPP_{branch}$, $ANPP_{foliage}$, $BNPP$, R_{eco}, R_{root}, R_{soil}, and $R_{het-soil}$. For two of the variables without significant differences among biomes ($ANPP_{litterfall}$ and $BNPP_{fine}$; Figs. S12 and S15, respectively), the same general trends applied but were not statistically significant. Another exception was for $BNPP_{root-coarse}$, where all records came from high-biomass forests in the US Pacific Northwest, resulting in marginally higher values for the temperate conifer biome (Table 1, Fig. S14; differences significant in mixed effects model but not in post-hoc pairwise comparison).

The most notable exception to the pattern of decreasing flux per unit area from tropical to boreal biomes was NEP, with no significant differences across biomes but with the largest average in temperate broadleaf forests, followed by tropical, boreal, and temperate conifer forests (Figs. 7, `rNEP_fig`).
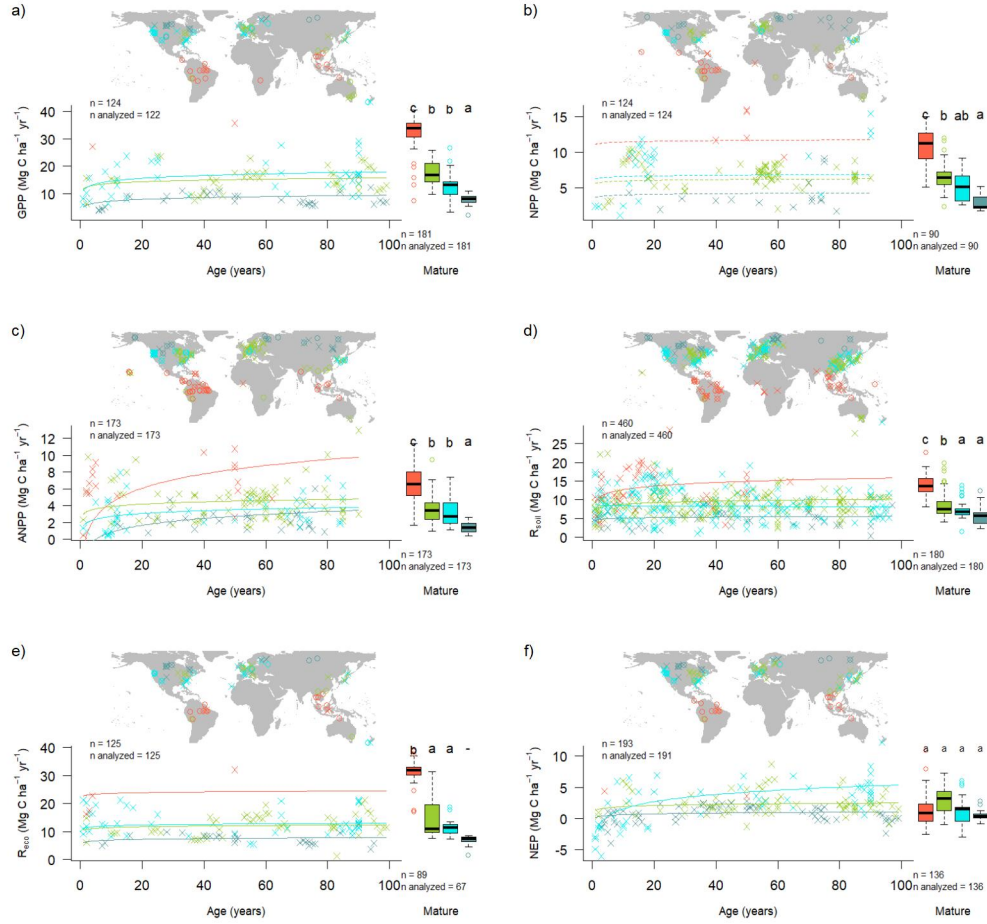
Figure 7 | Age trends and biome differences in some of the major C fluxes: (a) GPP, (b) NPP, (c) $ANPP$, (d) R_{soil}, (e) R_{eco}, and (f) NEP. Map shows data sources (x and o indicate young and mature stands, respectively). In each panel, the left scatterplot shows age trends in forests up to 100 years old, as characterized by a linear mixed effects model with fixed effects of age and biome. The fitted line indicates the effect of age on flux (solid lines: significant at p<0.05, dashed lines: non-significant), and non-parallel lines indicate a significant age x biome interaction. The boxplot illustrates distribution across mature forests, with different letters indicating significant differences between biomes. Data from biomes that did not meet the sample size criteria (see Methods) are plotted, but lack regression lines (young forests) or test of differences across biomes (mature forests). Individual figures for each flux with sufficient data are given in the Supplement (Figs. S4-S19).

268   There were sufficient data to assess mature forest biome differences for nine stock variables, and significant

269   differences among biomes were detected for five variables (B_{tot}, B_{ag}, $B_{ag-wood}$, $B_{foliage}$, $B_{root-coarse}$; Table

270   1). C stocks had less consistent patterns across biomes (Figs. 8, S20-S30). For B_{tot} and B_{ag}, tropical

271   broadleaf forests had the highest biomass and boreal forests the lowest, with temperate broadleaf and

272   needleleaf (B_{ag} only) intermediate. For three variables that had been disproportionately sampled in the

273   high-biomass forests of the US Pacific Northwest ($B_{ag-wood}$, $B_{foliage}$, and $B_{root-coarse}$), temperate conifer

274   forests had significantly higher stocks than the other biomes, which were not significantly different from one
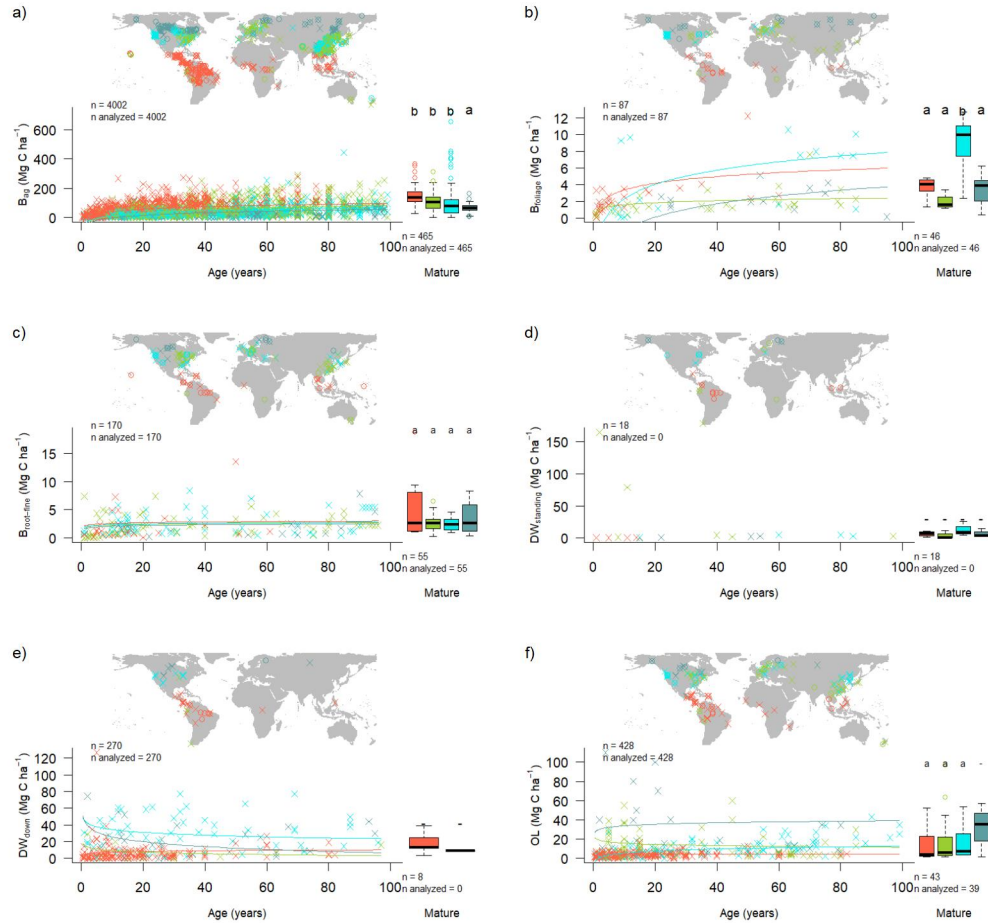
275   another.

16

Figure 8 | Age trends and biome differences in some of the major forest C stocks: (a) aboveground biomass, (b) foliage, (c) fine roots, (d) dead wood. Map shows data sources (x and o indicate young and mature stands, respectively). In each panel, the left scatterplot shows age trends in forests up to 100 years old, as characterized by a linear mixed effects model with fixed effects of age and biome. The fitted line indicates the effect of age on flux (solid lines: significant at $p<0.05$, dashed lines: non-significant), and non-parallel lines indicate a significant age x biome interaction. The boxplot illustrates distribution across mature forests, with different letters indicating signifant differences between biomes. Data from biomes that did not meet the sample size criteria (see Methods) are plotted, but lack regression lines (young forests) or test of differences across biomes (mature forests). Individual figures for each stock with sufficient data are given in the Supplement (Figs. S20-S30).

C cycling in young forests

Average C cycles for forests <100 years old are presented in Figures 8-11. Both C stocks and fluxes commonly increased significantly with stand age (Tables 1, S2, Figs. 7- 8, S5-S30; detailed below).

ForC contained 16 C flux variables with sufficient data for analyses of age trends in young forests (see Methods) (Figs. 7, S5-S19). Of these, ten increased significantly with age: NEP, GPP, $ANPP$, $ANPP_{woody}$, $ANPP_{foliage}$, $ANPP_{litterfal}$, $BNPP$, $BNPP_{fine}$, R_{eco}, and R_{root}. The remaining six–NPP, $ANPP_{stem}$, $ANPP_{branch}$, $BNPP_{coarse}$, $R_{soil-het}$, and $R_{soil-het}$–displayed no significant relationship to stand age.

Differences in C fluxes across biomes typically paralleled those observed for mature forests, with C cycling generally most rapid in the tropics and slowest in boreal forests. The single exception was $ANPP_{stem}$, for which temperate broadleaf and conifer forests had similar flux rates than tropical forests. Notably, and in

17

contrast to the lack of biome differences in NEP for mature forests (Fig. 7), the tendency for temperate forests to have greater fluxes than boreal forests held for NEP in regrowth forests (tropical forests excluded because of insufficient data).

In terms of C stocks, ten variables (all but standing deadwood, $DW_{standing}$) had sufficient data to test for age trends (Table 1, Figs. 8, S20-S30). All of these displayed a significant overall increase with with $log10[stand.age]$. There were sufficient data to model age $\times$ biome interactions were also significant for all ten of these C stock variables (Table S2), with living C stocks tending to accumulate more rapidly during the early stages of forest regrowth in tropical forests (Figs. 8, S20-S30). In the case of two non-living C stocks (DW_{down} and OL), age $\times$ biome interactions were such that Specifically, DW_{down} declined with age in temperate and boreal forests, compared to an increase with age in tropical forests (Figs. 8, S29). Similarly, OL declined slightly with age in temperate broadleaf forests, contrasting an increase in the other three biomes (Figs. 8, S30).

Discussion

ForC v3.0 provided unprecedented coverage of most major variables, yielding an internally consistent picture of C cycling in the world's major forest biomes. Carbon cycling rates generally increased from boreal to tropical regions and with stand age. Specifically, the major C fluxes were highest in tropical forests, intermediate in temperate (broadleaf or conifer) forests, and lowest in boreal forests – a pattern that generally held for regrowth as well as mature forests (Figs. 7- 8). In contrast to C fluxes, there was little directional variation in mature forest C stocks across biomes (Figs. 2-5, 8). The majority of flux variables, together with most live biomass pools, increased significantly with stand age (Table 1; Figs. 7- 8, S5-S30). Together, these results indicate that, moving from cold to tropical climates and from young to old stands, there is a general acceleration of C cycling, whereas C stocks and NEP of mature forests are correlated with a different set of factors.

C variable coverage and budget closure

The large number of C cycle variables covered by ForC, and the general consistency between them, provide confidence that our overall reported means provide accurate and useful baselines for analysis – with the caveats that they are unlikely to be accurate representations of C cycling for any particular forest, and that these sample means almost certainly do not represent true biome means (particularly for temperate conifer forests where high-biomass stands are over-represented in *ForC*).

There are of course notable holes in the ForC variable coverage (Fig. 2) that limit the scope of our inferences here. Notably, *ForC* currently has sparse–if any–coverage of fluxes to herbivores and higher consumers, along with the woody mortality (M_{woody}) and dead wood stocks (Table 1, Figs. S27-S29). Geographically, all variables are poorly covered in Africa and Siberia, a common problem in the carbon-cycle community (Xu and Shang 2016, **???**). *ForC* does not include soil carbon, which is covered by other efforts (e.g., Köchy *et al* 2015). *ForC* is not intended to replace databases that are specialized for particular parts of the C cycle analyses, e.g., aboveground biomass (Spawn *et al* 2020), land-atmosphere fluxes (Baldocchi *et al* 2001), soil respiration (Jian *et al* 2020), or the human footprint in global forests (**???**).

In this analysis, the C cycle budgets for mature forests (Figs. 3-6) generally "close"—that is, the sums of component variables do not differ from the larger fluxes by more than one standard deviation. On the one hand, this reflects the general fact that ecosystem-scale measurements tend to close the C budget more easily and consistently than, for example, for energy balance (Stoy *et al* 2013). On the other, however, *ForC* derives data from multiple heterogeneous sources, and standard deviations within each biome are high; as a result, the standard for C closure is relatively loose (*c.f.* Houghton 2020). Nonetheless, the lack of closure, in the one instance where it occurs, is probably more reflective of differences in the representation of forest types (*i.e.*, disproportionate representation of US Pacific NW for $B_{root-coarse}$ relative to B_{root}; Fig. 5) than of methodological accuracy. The overall high degree of closure implies that *ForC* gives a consistent picture of C cycling within biomes. This is an important and useful test, because it allows for consistency checks within the C cycle, for example leveraging separate and independently-measured fluxes to constrain errors in another (Phillips *et al* 2017, Williams *et al* 2014, Harmon *et al* 2011), or producing internally consistent global data products (Wang *et al* 2018).

C cycling across biomes

Our analysis reveals that carbon cycling is most rapid in the tropics and slowest in boreal regions, including C fluxes into (GPP), within (e.g., NPP and its components), and out of (e.g., R_{soil}, R_{eco}) the ecosystem. For mature forests, this is consistent with a large body of previous work demonstrating that C fluxes generally decline with latitude (or increase with temperature) on a global scale (e.g., Luyssaert *et al* 2007, Gillman *et al* 2015, Li and Xiao 2019, Banbury Morgan *et al* n.d.). The consistency with which this occurs across numerous fluxes is not surprising, but has never been simultaneously assessed across such a large number of variables (but see Banbury Morgan *et al* n.d. for nine autotrophic fluxes).

The notable exception to the pattern of fluxes decreasing from tropical to boreal regions is NEP (Fig. 7), which showed no significant differences across biomes. Unlike the other C flux variables, NEP does not characterize the rate at which C cycles through the ecosystem, but is the balance between C sequestration (GPP) and respiratory losses (R_{eco}) and represents net CO_2 sequestration (or release) by the ecosystem. NEP tends to be relatively small in mature forest stands (discussed further below), which accumulate carbon slowly relative to younger stands, if at all (Luyssaert *et al* 2008, **???**, Besnard *et al* 2018). It is therefore unsurprising that there are no pronounced differences across biomes, suggesting that variation in NEP of mature forests is controlled less by climate and more by other factors including moderate disturbances (**???**) or disequilibrium of R_{soil} relative to C inputs (e.g., in peatlands where anoxic conditions inhibit decomposition; Wilson *et al* 2016).

In contrast to the patterns observed for NEP in mature stands, NEP of stands between 20 and 100 years of age varied across biomes, being lowest in boreal forests, intermediate in temperate broadleaf forests, and highest in temperate conifer forests (with insufficient data to assess tropical forests; Figs. 7, S5). This is consistent with findings that live biomass accumulation rates (*e.g.*, ΔB_{ag} or ΔB_{tot}) during early secondary succession decrease with latitude (Figs. 7a, S16-S22; Anderson *et al* 2006, Cook-Patton *et al* 2020). Note, though, that NEP includes not only ΔB_{tot}, but also changes in DW_{tot}, OL, and soil carbon, and biome differences in the accumulation rates of these variables have not been detected, in part because these variables do not consistently increase with stand age (Figs. 8, S27-`r_OL_fig`, and see discussion below; Cook-Patton *et al* 2020).

For regrowth forests, little is known about cross-biome differences in carbon fluxes, and we are not aware of any previous large-scale comparisons of C fluxes that have been limited to regrowth forests. Thus, this analysis was the first to examine flux trends in regrowth forests across biomes. The observed tendency for young forest fluxes to decrease from tropical to boreal regions paralleled patterns in mature forests (Figs. 7, S5-S19), suggesting that regrowth forests follow latitudinal trends in carbon cycling similar to those of mature forests (e.g., Banbury Morgan *et al* n.d.).

In contrast to C fluxes and biomass accumulation rates in regrowth forests, stocks showed less systematic variation across biomes. For aboveground biomass, which is the variable in *ForC* with broadest geographical representation, the modest trend of declining biomass from tropical to boreal regions mirrors observations from spaceborne lidar that reveal a decline in aboveground biomass (for all forests, including secondary) with latitude across the N hemisphere (Hu *et al* 2016). The highest- biomass forests on Earth are, however, found in coastal temperate climates of both the southern and northern hemisphere (Keith *et al* 2009, Smithwick *et al* 2002, Hu *et al* 2016). Disproportionate representation of forests in one such region–the US Pacific Northwest–inflated estimates of temperate conifer fluxes and stocks for some variables and was responsible

378 for all of the anomalous results described here (e.g., lack of complete C budget closure, anomalous trend
379 across biomes for $BNPP_{coarse}$). Thus, biome differences should always be interpreted relative to the
380 geographic distribution of sampling, which only rarely covers the majority of forested area within a biome.

381 Whereas biomass can be remotely sensed and receives significant research attention, far less is known about
382 geographical variation in deadwood and organic layer (OL) across biomes, which has proved a limitation for
383 C accounting efforts (Pan *et al* 2011). Although these stocks can be important–exceeding 100 Mg C ha^{-1} in
384 some stands (Figs. 8, S27-S29), this study is the first to synthesize deadwood data on a global scale (but see
385 Cook-Patton *et al* 2020 for young forests). Unfortunately, data remain too sparse for statistical comparison
386 across biomes (Figs. 8, S27-S29; but see below for age trends), pointing to a need for more widespread
387 quantification of both standing and downed deadwood. *ForC* coverage of OL stocks is more comprehensive,
388 revealing no significant differences across temperate and tropical biomes, but a tendency towards higher OL
389 in boreal forests, consistent with the idea that slower decomposition in colder climates results in more
390 buildup of organic matter (Allen *et al* 2002). Further research on non-living C stocks in the world's forests
391 will be essential to completing the picture.

Age trends in C cycling

393 Our study reveals that most C fluxes quickly increase to a plateau as stands age (Fig. 7), consistent with
394 current understanding of age trends in forest C cycling (e.g., Anderson-Teixeira *et al* 2013, **???**, **???**). While
395 limited records in very young (*i.e.*, <5 year old) stands resulted in poor resolution of the earliest phases of
396 this increase for many variables (sometimes detecting no age trend; Table 1), any autotrophic C flux (e.g.,
397 GPP, NPP and its components, R_auto) would be minimal immediately following a stand-clearing
398 disturbance. These would be expected to increase rapidly with the most metabolically active components of
399 biomass, foliage and fine roots, which also increase rapidly with stand age (Fig. 8). In contrast, soil
400 heterotrophic respiration ($R_{het-soil}$) and total soil respiration (R_{soil}) are expected to be non-zero following
401 stand-clearing disturbance, although these may decrease with a reduction of root respiration (R_{soil} only) and
402 C exudates or increase in response to an influx of dead roots and litter (Ribeiro-Kumara *et al* 2020, Maurer
403 *et al* 2016, **???**). In this study, we detect no significant age trends in either variable.

404 Notably, net carbon sequestration (NEP) increases with age up to the 100-yr threshold examined here, with
405 more pronounced patterns in temperate than boreal forests (Fig. 7). This finding is largely consistent with,
406 but built from a far larger dataset than, previous studies showing an increase in NEP across relatively
407 young stand ages (Pregitzer and Euskirchen 2004, Baldocchi *et al* 2001, Luyssaert *et al* 2008). However,
408 NEP has been observed to decline from intermediate to old stands (Luyssaert *et al* 2008), and the NEP
409 estimated by our model for 100-year-old temperate conifer stands (~5 Mg C ha^{-1} yr^{-1}) exceeds the mean of
410 mature forests in the same biome (0.7 Mg C ha^{-1} yr^{-1}; Fig. 5). A decrease in NEP is consistent with the
411 observed deceleration of biomass accumulation as stands age, although both biomass and non-living C stocks
412 will often continue to increase well beyond the 100-yr threshold used here to delimit young and mature
413 stands (Luyssaert *et al* 2008, McGarvey *et al* 2014, Lichstein *et al* 2009).

414 In terms of stocks, our study reveals consistent increases in live biomass stocks with stand age–a pattern that
415 is well-known and expected (e.g., Lichstein *et al* 2009, Yang *et al* 2011)–and more variable age trends in
416 deadwood and OL. The latter are particularly sensitive to the type of disturbance, where disturbances that
417 remove most organic material (e.g., logging, agriculture) result in negligible deadwood in young stands,
418 followed by a buildup over time (tropical stands in Fig. 8; e.g., Vargas *et al* 2008). In contrast, natural

21

419 disturbances (e.g., fire, drought) can produce large amounts of deadwood (mostly $DW_{standing}$) that slowly
420 decomposes as the stand recovers, resulting in declines across young stand ages (e.g., temperate and boreal
421 stands in Fig. 8; e.g., Carmona *et al* 2002). Again, further study and synthesis of non-living C stocks across
422 biomes and stand ages will be valuable to giving a more comprehensive picture.

Relevance for climate change prediction and mitigation

424 The future of forest C cycling (Song *et al* 2019) will shape trends in atmospheric CO_2 and the course of
425 climate change (**???**). Our findings, and more generally the data contained in *ForC* and summarized here,
426 can help to meet two major challenges.

427 First, improved representation of forest C cycling in models is essential to improving predictions of the future
428 course of climate change, for the simple reason that by definition future projections extend our existing
429 observations and understanding to conditions that do not currently exist on Earth (McDowell *et al* 2018,
430 Bonan and Doney 2018, Gustafson *et al* 2018). To ensure that models are giving the right answers for the
431 right reasons (Sulman *et al* 2018), it is important to benchmark against multiple components of the C cycle
432 that are internally consistent with each other (Collier *et al* 2018, Wang *et al* 2018). *ForC*'s tens of thousands
433 of records are readily available in a standardized format, and our analyses here indicate that their internal
434 consistency is reasonably high. Integration of *ForC* with models will be valuable to improving the accuracy
435 and reliability of models.

436 Second, *ForC* can serve as a pipeline through which information can flow efficiently from forest researchers to
437 decision-makers working to implement forest conservation strategies at global, national, or landscape scales.
438 This is already happening: *ForC* has contributed to updating the IPCC guidelines for carbon accounting in
439 forests (IPCC 2019, Requena Suarez *et al* 2019), mapping C accumulation potential from natural forest
440 regrowth globally (Cook-Patton *et al* 2020), and informing ecosystem conservation priorities (Goldstein *et al*
441 2020).

442 It is also interesting to consider the complementary utility of global-scale but spatially discontinuous
443 databases such as ForC and remote wall-to-wall remote sensing products. The latter provide unparalleled
444 insight into aboveground carbon stocks, but less constraint on belowground stocks or carbon fluxes in general
445 (Bond-Lamberty *et al* 2016, Anav *et al* 2015). Combining observational data and remote observations may
446 provide a much more comprehensive and accurate picture of global forest C cycling, particularly when used
447 in formal data assimilation systems (Konings *et al* 2019, Liu *et al* 2018). Biomass is the largest C stock in
448 most forests, and most of the emphasis has traditionally been on this variable. Remote-sensing driven
449 biomass estimates (e.g., Saatchi *et al* 2011), calibrated based on high-quality ground-based data
450 (Schepaschenko *et al* 2019, **???**), are well suited for this task. Note, however, that factors such as stand age
451 and disturbance history are difficult, if possible, to detect remotely, and can only be characterized for very
452 recent decades (**???**, **???**, **???**). Ground-based data such as *ForC* are therefore valuable in defining
453 age-based trajectories in biomass, as in Cook-Patton *et al* (2020), and thus constraining variables such as
454 carbon sink potential (Luyssaert *et al* 2008).

455 In contrast, carbon allocation within forest ecosystems and respiration fluxes cannot be remotely sensed.
456 Efforts such as the Global Carbon Project (Friedlingstein *et al* 2019) and NASA's Carbon Monitoring
457 System (Liu *et al* 2018) typically compute respiration as residuals of all other terms (Bond-Lamberty *et al*
458 2016, Harmon *et al* 2011). This means that the errors on respiration outputs are likely to be large and

certainly poorly constrained, offering a unique opportunity for databases such as ForC and SRDB (Jian *et al* 2020) to provide observational benchmarks. For example, Konings *et al* (2019) produced a unique top-down estimate of global heterotrophic respiration that can both be compared with extant bottom-up estimates (Bond-Lamberty 2018) and used as an internal consistency check on other parts of the carbon cycle (Phillips *et al* 2017).

Conclusions

As climate change accelerates, understanding and managing the carbon dynamics of forests–notably including dynamics and fluxes that cannot be observed by satellites–is critical to forecasting, mitigation, and adaptation. The C data in *ForC*, as summarized here, will be valuable to these efforts. Notably, the fact that tropical forests tend to have both the highest rates of C sequestration in young stands (Fig. 8; Cook-Patton *et al* 2020), fueled by their generally high C flux rates (Table 1; Fig. 7), and the highest mean biomass (Fig. 8; Table 1; Hu *et al* 2016, Jian *et al* 2020) reinforces the concept that conservation and restoration of these forests is a priority for climate change mitigation, along with high-biomass old-growth temperate stands (Grassi *et al* 2017, Goldstein *et al* 2020). It is also important to note the trade-off in climate mitigation potential of restoration of young forests, with high rates of CO_2 sequestration (NEP; Cook-Patton *et al* 2020), versus conservation and management of mature forests, with low NEP but high C stocks that could not be recovered on a time scale relevant to climate change mitigation (Goldstein *et al* 2020). Generally speaking, the conservation of mature forests will yield greater climate benefits (Anderson-Teixeira and DeLucia 2011), but both approaches are critical to avoiding catastrophic climate change (IPCC 2018).

Acknowledgements

Data availability statement

Materials required to fully reproduce these analyses, including data, R scripts, and image files, are archived in Zenodo (DOI: TBD]. Data, scripts, and results presented here are also available through the open-access *ForC* GitHub repository (https://github.com/forc-db/ForC), where many will be updated as the database develops.

References

Allen A, Brown J and Gillooly J 2002 Global biodiversity, biochemical kinetics, and the energetic-equivalence rule *SCIENCE* **297** 1545–8

Anav A, Friedlingstein P, Beer C, Ciais P, Harper A, Jones C, Murray-Tortarolo G, Papale D, Parazoo N C, Peylin P, Piao S, Sitch S, Viovy N, Wiltshire A and Zhao M 2015 Spatiotemporal patterns of terrestrial gross primary production: A review *Reviews of Geophysics* **53** 785–818

Anderson K J, Allen A P, Gillooly J F and Brown J H 2006 Temperature-dependence of biomass accumulation rates during secondary succession *Ecology Letters* **9** 673–82

Anderson-Teixeira K, Herrmann V, CookPatton, Ferson A and Lister K 2020 Forc-db/GROA: Release with Cook-Patton et al. 2020, Nature.

Anderson-Teixeira K J, Davies S J, Bennett A C, Gonzalez-Akre E B, Muller-Landau H C, Joseph Wright S, Abu Salim K, Almeyda Zambrano A M, Alonso A, Baltzer J L, Basset Y, Bourg N A, Broadbent E N, Brockelman W Y, Bunyavejchewin S, Burslem D F R P, Butt N, Cao M, Cardenas D, Chuyong G B, Clay K, Cordell S, Dattaraja H S, Deng X, Detto M, Du X, Duque A, Erikson D L, Ewango C E N, Fischer G A, Fletcher C, Foster R B, Giardina C P, Gilbert G S, Gunatilleke N, Gunatilleke S, Hao Z, Hargrove W W, Hart T B, Hau B C H, He F, Hoffman F M, Howe R W, Hubbell S P, Inman-Narahari F M, Jansen P A, Jiang M, Johnson D J, Kanzaki M, Kassim A R, Kenfack D, Kibet S, Kinnaird M F, Korte L, Kral K, Kumar J, Larson A J, Li Y, Li X, Liu S, Lum S K Y, Lutz J A, Ma K, Maddalena D M, Makana J-R, Malhi Y, Marthews T, Mat Serudin R, McMahon S M, McShea W J, Memiaghe H R, Mi X, Mizuno T, Morecroft M, Myers J A, Novotny V, de Oliveira A A, Ong P S, Orwig D A, Ostertag R, den Ouden J, Parker G G, Phillips R P, Sack L, Sainge M N, Sang W, Sri-ngernyuang K, Sukumar R, Sun I-F, Sungpalee W, Suresh H S, Tan S, Thomas S C, Thomas D W, Thompson J, Turner B L, Uriarte M, Valencia R, et al 2015 CTFS-ForestGEO : A worldwide network monitoring forests in an era of global change *Global Change Biology* **21** 528–49

Anderson-Teixeira K J and DeLucia E H 2011 The greenhouse gas value of ecosystems *Global Change Biology* **17** 425–38

Anderson-Teixeira K J, Miller A D, Mohan J E, Hudiburg T W, Duval B D and DeLucia E H 2013 Altered dynamics of forest recovery under a changing climate *Global Change Biology* **19** 2001–21

Anderson-Teixeira K J, Wang M M H, McGarvey J C, Herrmann V, Tepley A J, Bond-Lamberty B and LeBauer D S 2018 ForC : A global database of forest carbon stocks and fluxes *Ecology* **99** 1507–7

Anderson-Teixeira K J, Wang M M H, McGarvey J C and LeBauer D S 2016 Carbon dynamics of mature and regrowth tropical forests derived from a pantropical database (TropForC-db) *Global Change Biology* **22** 1690–709

Badgley G, Anderegg L D L, Berry J A and Field C B 2019 Terrestrial gross primary production: Using NIRV to scale from site to globe *Global Change Biology* **25** 3731–40

Baldocchi D, Falge E, Gu L, Olson R, Hollinger D, Running S, Anthoni P, Bernhofer C, Davis K, Evans R, Fuentes J, Goldstein A, Katul G, Law B, Lee X, Malhi Y, Meyers T, Munger W, Oechel W, Paw K T, Pilegaard K, Schmid H P, Valentini R, Verma S, Vesala T, Wilson K and Wofsy S 2001 FLUXNET : A New Tool to Study the Temporal and Spatial Variability of EcosystemScale Carbon Dioxide, Water Vapor, and Energy Flux Densities *Bulletin of the American Meteorological Society* **82** 2415–34

Banbury Morgan B, Herrmann V, Kunert N, Bond-Lamberty B, Muller-Landau H C and Anderson-Teixeira K J Global patterns of forest autotrophic carbon fluxes *Global Change Biology*

Bates D, Mächler M, Bolker B and Walker S 2015 Fitting Linear Mixed-Effects Models Using **Lme4** *Journal of Statistical Software* **67**

Besnard S, Carvalhais N, Arain M A, Black A, de Bruin S, Buchmann N, Cescatti A, Chen J, Clevers J G P W, Desai A R, Gough C M, Havrankova K, Herold M, Hörtnagl L, Jung M, Knohl A, Kruijt B, Krupkova L, Law B E, Lindroth A, Noormets A, Roupsard O, Steinbrecher R, Varlagin A, Vincke C and Reichstein

M 2018 Quantifying the effect of forest age in annual net forest carbon balance *Environmental Research Letters* **13** 124018

Bonan G B 2008 Forests and Climate Change: Forcings, Feedbacks, and the Climate Benefits of Forests *Science* **320** 1444–9

Bonan G B and Doney S C 2018 Climate, ecosystems, and planetary futures: The challenge to predict life in Earth system models *Science* **359**

Bonan G B, Lombardozzi D L, Wieder W R, Oleson K W, Lawrence D M, Hoffman F M and Collier N 2019 Model Structure and Climate Data Uncertainty in Historical Simulations of the Terrestrial Carbon Cycle (1850) *Global Biogeochemical Cycles* **33** 1310–26

Bond-Lamberty B 2018 New Techniques and Data for Understanding the Global Soil Respiration Flux *Earth's Future* **6** 1176–80

Bond-Lamberty B, Epron D, Harden J, Harmon M E, Hoffman F, Kumar J, David McGuire A and Vargas R 2016 Estimating heterotrophic respiration at large scales: Challenges, approaches, and next steps *Ecosphere* **7**

Bond-Lamberty B and Thomson A 2010 A global database of soil respiration data *Biogeosciences* **7** 1915–26

Carmona M R, Armesto J J, Aravena J C and Pérez C A 2002 Coarse woody debris biomass in successional and primary temperate forests in Chiloé Island, Chile *Forest Ecology and Management* **164** 265–75

Cavaleri M A, Reed S C, Smith W K and Wood T E 2015 Urgent need for warming experiments in tropical forests *Global Change Biology* **21** 2111–21

Collier N, Hoffman F M, Lawrence D M, Keppel-Aleks G, Koven C D, Riley W J, Mu M and Randerson J T 2018 The International Land Model Benchmarking (ILAMB) System: Design, Theory, and Implementation *Journal of Advances in Modeling Earth Systems* **10** 2731–54

Cook-Patton S C, Leavitt S M, Gibbs D, Harris N L, Lister K, Anderson-Teixeira K J, Briggs R D, Chazdon R L, Crowther T W, Ellis P W, Griscom H P, Herrmann V, Holl K D, Houghton R A, Larrosa C, Lomax G, Lucas R, Madsen P, Malhi Y, Paquette A, Parker J D, Paul K, Routh D, Roxburgh S, Saatchi S, van den Hoogen J, Walker W S, Wheeler C E, Wood S A, Xu L and Griscom B W 2020 Mapping carbon accumulation potential from global natural forest regrowth *Nature* **585** 545–50

Corman J R, Collins S L, Cook E M, Dong X, Gherardi L A, Grimm N B, Hale R L, Lin T, Ramos J, Reichmann L G and Sala O E 2019 Foundations and Frontiers of Ecosystem Science: Legacy of a Classic Paper (Odum 1969) *Ecosystems* **22** 1160–72

Di Vittorio A V, Shi X, Bond-Lamberty B, Calvin K and Jones A 2020 Initial Land Use/Cover Distribution Substantially Affects Global Carbon and Local Temperature Projections in the Integrated Earth System Model *Global Biogeochemical Cycles* **34**

FAO 2010 *Global Forest Resources Assessment 2010* (Rome, Italy: Food and Agriculture Organization of the United Nations)

Friedlingstein P, Cox P, Betts R, Bopp L, von Bloh W, Brovkin V, Cadule P, Doney S, Eby M, Fung I, Bala G, John J, Jones C, Joos F, Kato T, Kawamiya M, Knorr W, Lindsay K, Matthews H D, Raddatz T, Rayner P, Reick C, Roeckner E, Schnitzler K-G, Schnur R, Strassmann K, Weaver A J, Yoshikawa C and

Zeng N 2006 ClimateCarbon Cycle Feedback Analysis: Results from the C4MIP Model Intercomparison *Journal of Climate* **19** 3337–53

Friedlingstein P, Jones M W, O'Sullivan M, Andrew R M, Hauck J, Peters G P, Peters W, Pongratz J, Sitch S, Quéré C L, Bakker D C E, Canadell J G, Ciais P, Jackson R B, Anthoni P, Barbero L, Bastos A, Bastrikov V, Becker M, Bopp L, Buitenhuis E, Chandra N, Chevallier F, Chini L P, Currie K I, Feely R A, Gehlen M, Gilfillan D, Gkritzalis T, Goll D S, Gruber N, Gutekunst S, Harris I, Haverd V, Houghton R A, Hurtt G, Ilyina T, Jain A K, Joetzjer E, Kaplan J O, Kato E, Klein Goldewijk K, Korsbakken J I, Landschützer P, Lauvset S K, Lefèvre N, Lenton A, Lienert S, Lombardozzi D, Marland G, McGuire P C, Melton J R, Metzl N, Munro D R, Nabel J E M S, Nakaoka S-I, Neill C, Omar A M, Ono T, Peregon A, Pierrot D, Poulter B, Rehder G, Resplandy L, Robertson E, Rödenbeck C, Séférian R, Schwinger J, Smith N, Tans P P, Tian H, Tilbrook B, Tubiello F N, Werf G R van der, Wiltshire A J and Zaehle S 2019 Global Carbon Budget 2019 *Earth System Science Data* **11** 1783–838

Gillman L N, Wright S D, Cusens J, McBride P D, Malhi Y and Whittaker R J 2015 Latitude, productivity and species richness *Global Ecology and Biogeography* **24** 107–17

Goldstein A, Turner W R, Spawn S A, Anderson-Teixeira K J, Cook-Patton S, Fargione J, Gibbs H K, Griscom B, Hewson J H, Howard J F, Ledezma J C, Page S, Koh L P, Rockström J, Sanderman J and Hole D G 2020 Protecting irrecoverable carbon in Earth's ecosystems *Nature Climate Change* **10** 287–95

Grassi G, House J, Dentener F, Federici S, den Elzen M and Penman J 2017 The key role of forests in meeting climate targets requires science for credible mitigation *Nature Climate Change* **7** 220–6

Griscom B W, Adams J, Ellis P W, Houghton R A, Lomax G, Miteva D A, Schlesinger W H, Shoch D, Siikamäki J V, Smith P, Woodbury P, Zganjar C, Blackman A, Campari J, Conant R T, Delgado C, Elias P, Gopalakrishna T, Hamsik M R, Herrero M, Kiesecker J, Landis E, Laestadius L, Leavitt S M, Minnemeyer S, Polasky S, Potapov P, Putz F E, Sanderman J, Silvius M, Wollenberg E and Fargione J 2017 Natural climate solutions *Proceedings of the National Academy of Sciences* **114** 11645–50

Gustafson E J, Kubiske M E, Miranda B R, Hoshika Y and Paoletti E 2018 Extrapolating plot-scale CO2 and ozone enrichment experimental results to novel conditions and scales using mechanistic modeling *Ecological Processes* **7** 31

Harmon M E, Bond-Lamberty B, Tang J and Vargas R 2011 Heterotrophic respiration in disturbed forests: A review with examples from North America *Journal of Geophysical Research* **116**

Houghton R A 2020 Terrestrial fluxes of carbon in GCP carbon budgets *Global Change Biology* **26** 3006–14

Hu T, Su Y, Xue B, Liu J, Zhao X, Fang J and Guo Q 2016 Mapping Global Forest Aboveground Biomass with Spaceborne LiDAR, Optical Imagery, and Forest Inventory Data *Remote Sensing* **8** 565

IPCC 2019 *2019 Refinement to the 2006 IPCC Guidelines for National Greenhouse Gas Inventories*

IPCC 2018 *Global Warming of 1.5C. An IPCC Special Report on the impacts of global warming of 1.5C above pre-industrial levels and related global greenhouse gas emission pathways, in the context of strengthening the global response to the threat of climate change, sustainable development, and efforts to eradicate poverty [Masson-Delmotte, V., P. Zhai, H.-O. Pörtner, D. Roberts, J. Skea, P.R. Shukla, A. Pirani, W. Moufouma-Okia, C. Péan, R. Pidcock, S. Connors, J.B.R. Matthews, Y. Chen, X. Zhou, M.I. Gomis, E. Lonnoy, T. Maycock, M. Tignor, and T. Waterfield (eds.)].*

Jian J, Vargas R, Anderson-Teixeira K, Stell E, Herrmann V, Horn M, Kholod N, Manzon J, Marchesi R, Paredes D and Bond-Lamberty B 2020 *A restructured and updated global soil respiration database (SRDB-V5)* (Data, Algorithms, and Models)

Jung M, Henkel K, Herold M and Churkina G 2006 Exploiting synergies of global land cover products for carbon cycle modeling *Remote Sensing of Environment* **101** 534–53

Keith H, Mackey B G and Lindenmayer D B 2009 Re-evaluation of forest biomass carbon stocks and lessons from the world's most carbon-dense forests *Proceedings of the National Academy of Sciences* **106** 11635–40

Konings A G, Bloom A A, Liu J, Parazoo N C, Schimel D S and Bowman K W 2019 Global satellite-driven estimates of heterotrophic respiration *Biogeosciences* **16** 2269–84

Köchy M, Hiederer R and Freibauer A 2015 Global distribution of soil organic carbon Part 1: Masses and frequency distributions of SOC stocks for the tropics, permafrost regions, wetlands, and the world *SOIL* **1** 351–65

Krause A, Pugh T A M, Bayer A D, Li W, Leung F, Bondeau A, Doelman J C, Humpenöder F, Anthoni P, Bodirsky B L, Ciais P, Müller C, Murray-Tortarolo G, Olin S, Popp A, Sitch S, Stehfest E and Arneth A 2018 Large uncertainty in carbon uptake potential of land-based climate-change mitigation efforts *Global Change Biology* **24** 3025–38

Li X and Xiao J 2019 Mapping Photosynthesis Solely from Solar-Induced Chlorophyll Fluorescence: A Global, Fine-Resolution Dataset of Gross Primary Production Derived from OCO-2 *Remote Sensing* **11** 2563

Lichstein J W, Wirth C, Horn H S and Pacala S W 2009 Biomass Chronosequences of United States Forests: Implications for Carbon Storage and Forest Management *Old-Growth Forests* Ecological Studies ed C Wirth, G Gleixner and M Heimann (Springer Berlin Heidelberg) pp 301–41

Lieth H 1973 Primary production: Terrestrial ecosystems *Human Ecology* **1** 303–32

Liu J, Bowman K, Parazoo N C, Bloom A A, Wunch D, Jiang Z, Gurney K R and Schimel D 2018 Detecting drought impact on terrestrial biosphere carbon fluxes over contiguous US with satellite observations *Environmental Research Letters* **13** 095003

Lutz J A, Furniss T J, Johnson D J, Davies S J, Allen D, Alonso A, Anderson-Teixeira K J, Andrade A, Baltzer J, Becker K M L, Blomdahl E M, Bourg N A, Bunyavejchewin S, Burslem D F R P, Cansler C A, Cao K, Cao M, Cárdenas D, Chang L-W, Chao K-J, Chao W-C, Chiang J-M, Chu C, Chuyong G B, Clay K, Condit R, Cordell S, Dattaraja H S, Duque A, Ewango C E N, Fischer G A, Fletcher C, Freund J A, Giardina C, Germain S J, Gilbert G S, Hao Z, Hart T, Hau B C H, He F, Hector A, Howe R W, Hsieh C-F, Hu Y-H, Hubbell S P, Inman-Narahari F M, Itoh A, Janík D, Kassim A R, Kenfack D, Korte L, Král K, Larson A J, Li Y, Lin Y, Liu S, Lum S, Ma K, Makana J-R, Malhi Y, McMahon S M, McShea W J, Memiaghe H R, Mi X, Morecroft M, Musili P M, Myers J A, Novotny V, Oliveira A de, Ong P, Orwig D A, Ostertag R, Parker G G, Patankar R, Phillips R P, Reynolds G, Sack L, Song G-Z M, Su S-H, Sukumar R, Sun I-F, Suresh H S, Swanson M E, Tan S, Thomas D W, Thompson J, Uriarte M, Valencia R, Vicentini A, Vrška T, Wang X, Weiblen G D, Wolf A, Wu S-H, Xu H, Yamakura T, Yap S and Zimmerman J K 2018 Global importance of large-diameter trees *Global Ecology and Biogeography* **27** 849–64

Luyssaert S, Inglima I, Jung M, Richardson A D, Reichstein M, Papale D, Piao S L, Schulze E-D, Wingate L, Matteucci G, Aragao L, Aubinet M, Beer C, Bernhofer C, Black K G, Bonal D, Bonnefond J-M, Chambers J, Ciais P, Cook B, Davis K J, Dolman A J, Gielen B, Goulden M, Grace J, Granier A, Grelle A, Griffis T, Grünwald T, Guidolotti G, Hanson P J, Harding R, Hollinger D Y, Hutyra L R, Kolari P, Kruijt B, Kutsch W, Lagergren F, Laurila T, Law B E, Maire G L, Lindroth A, Loustau D, Malhi Y, Mateus J, Migliavacca M, Misson L, Montagnani L, Moncrieff J, Moors E, Munger J W, Nikinmaa E, Ollinger S V, Pita G, Rebmann C, Roupsard O, Saigusa N, Sanz M J, Seufert G, Sierra C, Smith M-L, Tang J, Valentini R, Vesala T and Janssens I A 2007 CO2 balance of boreal, temperate, and tropical forests derived from a global database *Global Change Biology* **13** 2509–37

Luyssaert S, Schulze E D, Borner A, Knohl A, Hessenmoller D, Law B E, Ciais P and Grace J 2008 Old-growth forests as global carbon sinks *Nature* **455** 213

Maurer G E, Chan A M, Trahan N A, Moore D J P and Bowling D R 2016 Carbon isotopic composition of forest soil respiration in the decade following bark beetle and stem girdling disturbances in the Rocky Mountains *Plant, Cell & Environment* **39** 1513–23

McDowell N G, Allen C D, Anderson-Teixeira K, Aukema B H, Bond-Lamberty B, Chini L, Clark J S, Dietze M, Grossiord C, Hanbury-Brown A, Hurtt G C, Jackson R B, Johnson D J, Kueppers L, Lichstein J W, Ogle K, Poulter B, Pugh T A M, Seidl R, Turner M G, Uriarte M, Walker A P and Xu C 2020 Pervasive shifts in forest dynamics in a changing world *Science* **368**

McDowell N G, Michaletz S T, Bennett K E, Solander K C, Xu C, Maxwell R M and Middleton R S 2018 Predicting Chronic Climate-Driven Disturbances and Their Mitigation *Trends in Ecology & Evolution* **33** 15–27

McGarvey J C, Thompson J R, Epstein H E and Shugart H H 2014 Carbon storage in old-growth forests of the Mid-Atlantic: Toward better understanding the eastern forest carbon sink *Ecology* **96** 311–7

Novick K A, Biederman J A, Desai A R, Litvak M E, Moore D J P, Scott R L and Torn M S 2018 The AmeriFlux network: A coalition of the willing *Agricultural and Forest Meteorology* **249** 444–56

Odum E 1969 The strategy of ecosystem development *Science* **164** 262–70

Pan Y, Birdsey R A, Fang J, Houghton R, Kauppi P E, Kurz W A, Phillips O L, Shvidenko A, Lewis S L, Canadell J G, Ciais P, Jackson R B, Pacala S, McGuire A D, Piao S, Rautiainen A, Sitch S and Hayes D 2011 A Large and Persistent Carbon Sink in the World's Forests *Science* **333** 988–93

Phillips C L, Bond-Lamberty B, Desai A R, Lavoie M, Risk D, Tang J, Todd-Brown K and Vargas R 2017 The value of soil respiration measurements for interpreting and modeling terrestrial carbon cycling *Plant and Soil* **413** 1–25

Pregitzer K S and Euskirchen E S 2004 Carbon cycling and storage in world forests: Biome patterns related to forest age *Global Change Biology* **10** 2052–77

Pugh T A M, Lindeskog M, Smith B, Poulter B, Arneth A, Haverd V and Calle L 2019 Role of forest regrowth in global carbon sink dynamics *Proceedings of the National Academy of Sciences* **116** 4382–7

Requena Suarez D, Rozendaal D M A, Sy V D, Phillips O L, Alvarez-Dávila E, Anderson-Teixeira K, Araujo-Murakami A, Arroyo L, Baker T R, Bongers F, Brienen R J W, Carter S, Cook-Patton S C,

Feldpausch T R, Griscom B W, Harris N, Hérault B, Coronado E N H, Leavitt S M, Lewis S L, Marimon B S, Mendoza A M, N'dja J K, N'Guessan A E, Poorter L, Qie L, Rutishauser E, Sist P, Sonké B, Sullivan M J P, Vilanova E, Wang M M H, Martius C and Herold M 2019 Estimating aboveground net biomass change for tropical and subtropical forests: Refinement of IPCC default rates using forest plot data *Global Change Biology* **25** 3609–24

Ribeiro-Kumara C, Köster E, Aaltonen H and Köster K 2020 How do forest fires affect soil greenhouse gas emissions in upland boreal forests? A review *Environmental Research* **184** 109328

Saatchi S S, Harris N L, Brown S, Lefsky M, Mitchard E T A, Salas W, Zutta B R, Buermann W, Lewis S L, Hagen S, Petrova S, White L, Silman M and Morel A 2011 Benchmark map of forest carbon stocks in tropical regions across three continents *Proceedings of the National Academy of Sciences* **108** 9899–904

Schepaschenko D, Chave J, Phillips O L, Lewis S L, Davies S J, Réjou-Méchain M, Sist P, Scipal K, Perger C, Herault B, Labrière N, Hofhansl F, Affum-Baffoe K, Aleinikov A, Alonso A, Amani C, Araujo-Murakami A, Armston J, Arroyo L, Ascarrunz N, Azevedo C, Baker T, Bałazy R, Bedeau C, Berry N, Bilous A M, Bilous S Y, Bissiengou P, Blanc L, Bobkova K S, Braslavskaya T, Brienen R, Burslem D F R P, Condit R, Cuni-Sanchez A, Danilina D, Torres D del C, Derroire G, Descroix L, Sotta E D, d'Oliveira M V N, Dresel C, Erwin T, Evdokimenko M D, Falck J, Feldpausch T R, Foli E G, Foster R, Fritz S, Garcia-Abril A D, Gornov A, Gornova M, Gothard-Bassébé E, Gourlet-Fleury S, Guedes M, Hamer K C, Susanty F H, Higuchi N, Coronado E N H, Hubau W, Hubbell S, Ilstedt U, Ivanov V V, Kanashiro M, Karlsson A, Karminov V N, Killeen T, Koffi J-C K, Konovalova M, Kraxner F, Krejza J, Krisnawati H, Krivobokov L V, Kuznetsov M A, Lakyda I, Lakyda P I, Licona J C, Lucas R M, Lukina N, Lussetti D, Malhi Y, Manzanera J A, Marimon B, Junior B H M, Martinez R V, Martynenko O V, Matsala M, Matyashuk R K, Mazzei L, Memiaghe H, Mendoza C, Mendoza A M, Moroziuk O V, Mukhortova L, Musa S, Nazimova D I, Okuda T, Oliveira L C, et al 2019 The Forest Observation System, building a global reference dataset for remote sensing of forest biomass *Scientific Data* **6** 1–11

Schimel D, Hargrove W, Hoffman F and MacMahon J 2007 NEON: A hierarchically designed national ecological network *Frontiers in Ecology and the Environment* **5** 59–9

Smithwick E A H, Harmon M E, Remillard S M, Acker S A and Franklin J F 2002 Potential upper bounds of carbon stores in forests of the Pacific Northwest *Ecological Applications* **12** 1303–17

Song J, Wan S, Piao S, Knapp A K, Classen A T, Vicca S, Ciais P, Hovenden M J, Leuzinger S, Beier C, Kardol P, Xia J, Liu Q, Ru J, Zhou Z, Luo Y, Guo D, Adam Langley J, Zscheischler J, Dukes J S, Tang J, Chen J, Hofmockel K S, Kueppers L M, Rustad L, Liu L, Smith M D, Templer P H, Quinn Thomas R, Norby R J, Phillips R P, Niu S, Fatichi S, Wang Y, Shao P, Han H, Wang D, Lei L, Wang J, Li X, Zhang Q, Li X, Su F, Liu B, Yang F, Ma G, Li G, Liu Y, Liu Y, Yang Z, Zhang K, Miao Y, Hu M, Yan C, Zhang A, Zhong M, Hui Y, Li Y and Zheng M 2019 A meta-analysis of 1,119 manipulative experiments on terrestrial carbon-cycling responses to global change *Nature Ecology & Evolution* **3** 1309–20

Spawn S A, Sullivan C C, Lark T J and Gibbs H K 2020 Harmonized global maps of above and belowground biomass carbon density in the year 2010 *Scientific Data* **7** 112

Stoy P C, Mauder M, Foken T, Marcolla B, Boegh E, Ibrom A, Arain M A, Arneth A, Aurela M, Bernhofer C, Cescatti A, Dellwik E, Duce P, Gianelle D, van Gorsel E, Kiely G, Knohl A, Margolis H, McCaughey H, Merbold L, Montagnani L, Papale D, Reichstein M, Saunders M, Serrano-Ortiz P, Sottocornola M,

729 Spano D, Vaccari F and Varlagin A 2013 A data-driven analysis of energy balance closure across

730 FLUXNET research sites: The role of landscape scale heterogeneity *Agricultural and Forest Meteorology*

731 **171-172** 137–52

732 Sulman B N, Moore J A M, Abramoff R, Averill C, Kivlin S, Georgiou K, Sridhar B, Hartman M D, Wang

733 G, Wieder W R, Bradford M A, Luo Y, Mayes M A, Morrison E, Riley W J, Salazar A, Schimel J P,

734 Tang J and Classen A T 2018 Multiple models and experiments underscore large uncertainty in soil

735 carbon dynamics *Biogeochemistry* **141** 109–23

736 Tubiello F N, Pekkarinen A, Marklund L, Wanner N, Conchedda G, Federici S, Rossi S and Grassi G 2020

737 Carbon Emissions and Removals by Forests: New Estimates 1990–2020 *Earth System Science*

738 *Data Discussions* 1–21

739 van der Werf G R, Randerson J T, Giglio L, van Leeuwen T T, Chen Y, Rogers B M, Mu M, van Marle M J

740 E, Morton D C, Collatz G J, Yokelson R J and Kasibhatla P S 2017 Global fire emissions estimates

741 during 1997 *Earth System Science Data* **9** 697–720

742 Vargas R, Allen M F and Allen E B 2008 Biomass and carbon accumulation in a fire chronosequence of a

743 seasonally dry tropical forest *Global Change Biology* **14** 109–24

744 Wang Y, Ciais P, Goll D, Huang Y, Luo Y, Wang Y-P, Bloom A A, Broquet G, Hartmann J, Peng S,

745 Penuelas J, Piao S, Sardans J, Stocker B D, Wang R, Zaehle S and Zechmeister-Boltenstern S 2018

746 GOLUM-CNP v1.0: A data-driven modeling of carbon, nitrogen and phosphorus cycles in major

747 terrestrial biomes *Geoscientific Model Development* **11** 3903–28

748 Warner D L, Bond-Lamberty B, Jian J, Stell E and Vargas R 2019 Spatial Predictions and Associated

749 Uncertainty of Annual Soil Respiration at the Global Scale *Global Biogeochemical Cycles* **33** 1733–45

750 Williams C A, Collatz G J, Masek J, Huang C and Goward S N 2014 Impacts of disturbance history on

751 forest carbon stocks and fluxes: Merging satellite disturbance mapping with forest inventory data in a

752 carbon cycle model framework *Remote Sensing of Environment* **151** 57–71

753 Wilson R M, Hopple A M, Tfaily M M, Sebestyen S D, Schadt C W, Pfeifer-Meister L, Medvedeff C,

754 McFarlane K J, Kostka J E, Kolton M, Kolka R K, Kluber L A, Keller J K, Guilderson T P, Griffiths N

755 A, Chanton J P, Bridgham S D and Hanson P J 2016 Stability of peatland carbon to rising temperatures

756 *Nature Communications* **7** 13723

757 Xu M and Shang H 2016 Contribution of soil respiration to the global carbon equation *Journal of Plant*

758 *Physiology* **203** 16–28

759 Yang Y, Luo Y and Finzi A C 2011 Carbon and nitrogen dynamics during forest stand development: A

760 global synthesis *New Phytologist* **190** 977